ELSEVIER

Chemical Physics 227 (1998) 83–98

Chemical Physics

Triplet exciton generation, transport and relaxation in isolated polydiacetylene chains: subpicosecond pump-probe experiments

B. Kraabel [a], D. Hulin [a], C. Aslangul [b], C. Lapersonne-Meyer [b,1], M. Schott [b,*]

[a] *Laboratoire d'Optique Appliquée, URA 1406 du CNRS, ENSTA — École Polytechnique, F-91125 Palaiseau Cedex, France*

[b] *Groupe de Physique des Solides, URA 040017 du CNRS, Universités Paris 6 et 7, 2 Place Jussieu, F-75251 Paris Cedex 05, France*

Received 4 June 1997

Abstract

Triplet states of 3- and 4-BCMU isolated polydiacetylene chains dispersed in their single-crystal monomer matrix are studied by subpicosecond pump-probe experiments. Triplet population is monitored by an intense and narrow TT^* photoinduced absorption band near 1.35 eV at 20 K. In our experimental conditions, we find that triplets are generated by two different processes: fission of singlets generated by the pump (1-quantum process); or fission of highly excited singlets produced by absorption of pump photons by the singlet exciton (2-quantum process). The lowest triplet lies slightly above half the singlet energy. Thus the final state T^* of the induced absorption is ≤ 0.1 eV below the known electron–hole generation gap. No clear evidence of self-trapping of the triplet exciton is observed. Triplet population decay is governed by diffusion of triplets on the chain (hopping rate $\approx 10^{11}$ s^{-1}) and efficient annihilation of triplet pairs at contact (rate $\approx 4 \times 10^{11}$ s^{-1}). It is also shown that this TT^* transition is very strong: one order of magnitude stronger than the ground state to singlet exciton transition. © 1998 Elsevier Science B.V.

1. Introduction

Polydiacetylenes (PDAs) are good model systems for the study of conjugated polymers, since they can be obtained as single crystals of macroscopic size by solid state topochemical polymerization of the corresponding diacetylene (DA) monomer crystal [1–3].

We study here diacetylene monomer single crystals containing chains of the corresponding polydiacetylene polymer at a concentration of $\sim 10^{-4}$ in weight. The chosen DAs are known as 3BCMU and 4BCMU whose side-groups are $-(CH_2)_n-OCO-NH-COOC_4H_9$, where $n = 3$ and 4 for 3BCMU and 4BCMU, respectively. Thermal polymerization of these DAs is negligible, so a constant and small polymer concentration can be maintained indefinitely in a sample. However, they readily polymerize under γ-ray irradiation [4]. The resulting chains are very long, ~ 2.6 μm, with a very small dispersion in length [4], and are thus good approximations of infinite chains. At a concentration $\sim 10^{-4}$ in weight, the average interchain distance is several tens of nanometers. Hence, interchain interactions can be neglected and each chain may be considered an isolated 1-D system. Moreover, in the crystalline monomer matrix, all the chains are perfectly aligned and parallel and have the same geometry and the

* Corresponding author.

[1] Also at: IUFM de l'Académie de Créteil, 94861 Bonneuil-sur-Marne Cedex, France.

PII S0301-0104(97)00200-0

same environment (surrounding monomer crystal): they are in fact 1-D crystals.

The lowest electronic excitation of these monomer molecules is the triplet of the diacetylene group at ~ 3 eV [5], and the lowest singlet state also belongs to the diacetylene group and is at ~ 4.6 eV [6]. Thus, any absorption in the visible and near UV range is entirely due to the polymer chains. Their absorption spectrum is dominated by an intense, narrow (fwhm 7.4 meV at low temperature) and highly dichroic line (dichroic ratio ≥ 250) [7] corresponding to the singlet ^1B_u exciton absorption which is referred to as S_1 below [8]. Fig. 1 shows the absorption of isolated chains of poly-4BCMU, peaking at ~ 14585 cm^{-1} or 1.81 eV at 15 K (solid line). In the case of 3BCMU, spectra are very similar except for a slightly higher exciton transition energy of the isolated chains, at ~ 15330 cm^{-1} or 1.90 eV.

Both poly-3BCMU and poly-4BCMU chains isolated in their respective monomer matrices exhibit a weak fluorescence [9], whereas bulk poly-4BCMU is considered to be non-fluorescent. Apart from the region of the main exciton transition where emitted light is reabsorbed, the emission spectrum shown in Fig. 1 (dashed line) is essentially a mirror image of the exciton absorption with no Stokes shift. The emission origin coincides with the main exciton absorption energy to the experimental accuracy of a few cm^{-1}.

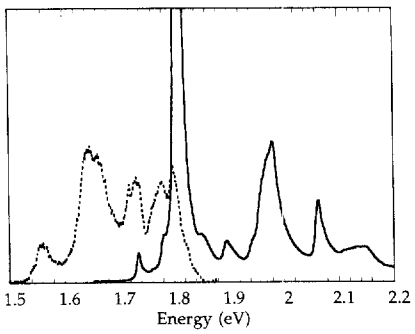

Fig. 1. Absorption (solid line) and emission (dashed line) spectra at 15 K of poly-4BCMU chains in their single crystal monomer matrix. The singlet exciton absorption S_1 peaks at 1.81 eV. Emission is produced by excitation at 514.5 nm. The emission is reabsorbed in the region of the exciton absorption (it is not corrected for the detector sensitivity, which decreases below 1.6 eV and becomes zero below ~ 1.5 eV).

The nature and relaxation processes of electronic excitations of these chains are studied with the goal of providing generic information about conjugated polymers in general. We have studied these processes via photobleaching and photoinduced absorption by subpicosecond pump-probe experiments. Information concerning both the singlet and triplet manifold is obtained. Since the singlet exciton of such isolated chains is fluorescent, its relaxation may also be studied by up-conversion measurements of the emission. This study yielded a decay time (i.e., a singlet exciton lifetime) of the order of 200 fs. The exciton relaxes essentially via non-radiative processes. Results on the singlet relaxation will be reported elsewhere [10,11].

This paper deals with triplet formation and relaxation. Contrary to the singlet relaxation, which has been extensively studied (e.g., [12–14]), less is known in the case of the triplet states. Triplets in PDAs have almost always been studied by monitoring the induced TT^* absorption around 900 nm [15–18]. Lifetimes of 50–100 μs have been observed and the triplet magnetic structure has been determined [16,19,20].

In this work as well the triplet population is monitored via TT^* absorption intensity. The experimental setup is described in Section 2. Experimental results are presented in Section 3: we studied the dependence of the triplet yield with pump fluence and pump photon energy, and the temporal decay of the triplet population. Using these results, we discuss (Section 4) possible triplet generation processes, the energy of the lowest triplet state, triplet transport properties (see theoretical treatment in Appendix A), the possible occurrence of selftrapping, the position of the higher lying T^* state and the strength of the TT^* transition.

2. Experimental setup

The laser system consists of a Coherent RegA Ti:Sapphire oscillator amplified by a Coherent Mira regenerative amplifier, and delivers 4 μJ, 150 fs, 800 nm linearly polarized pulses at a repetition rate of 250 kHz. This pulse train is split into two beams, as shown schematically in Fig. 2, which are used as

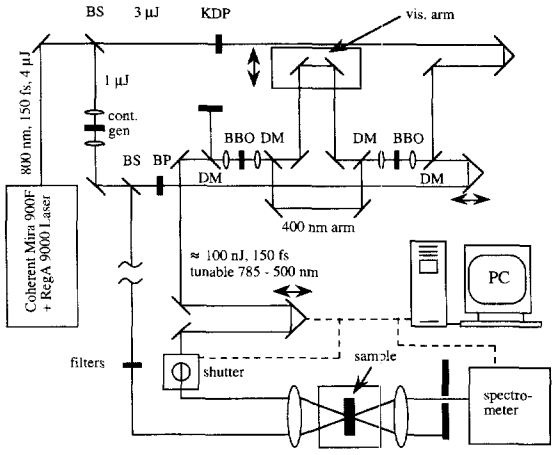

Fig. 2. A schematic diagram of the experimental arrangement. The elements labeled *BS* are beam-splitters, *DM* are dichroic mirrors, *BP* filter is a variable 15 nm bandpass filter and *cont. gen.* is the sapphire plate and focusing lenses which constitute the continuum generator.

input to a type I visibly-pumped OPA. The beam used to pump the OPA consists of 3 μJ pulses, and is frequency-doubled in a 1 mm thick KDP crystal. The other beam is focused into a sapphire plate to generate a white-light continuum to serve as seed pulses for the OPA (before entering the OPA a small portion of the continuum is split off to serve as the probe beam). Prior to amplification, the continuum is filtered using a variable 15 nm bandpass filter to ensure that the output of the OPA has a negligible white-light background. The spectrally narrow seed pulses are then amplified in a two-stage OPA using a collinear geometry, with a 1 mm thick BBO crystal in the first stage and a 2 mm thick BBO crystal in the second stage. Typical pulse widths for the output of the OPA are 150 fs, with the pulse-to-pulse stability better than 10% as measured by a fast photo-diode.

The output of the OPA serves as the pump beam and passes through an optical delay line after which it is focused on the sample. The probe beam, focused on the sample at the same spot as the pump beam, is transmitted through the sample and monitored using a CCD detector mounted on a spectrometer. The stability of the laser system enables us to achieve an excellent signal-to-noise ratio without using a reference beam. The probe spectrum is measured with and without the pump (I_{on} and I_{off}, respectively) at a 12 Hz repetition rate. The differential absorption signal, $-\Delta\alpha d = \ln[I_{on}(\omega)/I_{off}(\omega)]$, is then recorded as a function of the time delay between the pump and the probe pulse, providing a time-resolved measurement of the transmission dynamics of the sample subsequent to its excitation by the pump pulse.

In order to calculate the excitation densities we measure the horizontal diameter of the beam spots by translating a 5 μm slit, mounted in the cryostat next to the samples, across the beam spots. The probe beam is focused on the sample to a circular spot of 50 μm diameter, and the pump beam is focused to a circular spot of 150–200 μm diameter, completely covering the probe beam spot. The high-quality spatial mode of the pump beam justified the assumption that the pump beam spot is circularly symmetric, which was confirmed through visual observation via a CCD camera. This also allows us to verify that the probe beam spot is essentially circularly symmetric. We optimize the horizontal overlap of the pump and probe spots on the sample by maximizing simultaneously their transmission through the slit. Vertical overlap is optimized visually via the CCD camera, and verified by maximizing the signal. In addition, the measurement of the spot size shows that there is no horizontal spatial chirp on the pump beam.

In addition to measuring the differential absorption spectrum as a function of time, we also measure it (for a given time) as a function of pump fluence. In order to determine the pump fluence we measure the pump power at the entrance of the cryostat immediately before and after measurement of the PIA spectrum, in order to verify that the power does not fluctuate significantly during accumulation of the data.

Single crystals of monomer 3 and 4BCMU are grown by slow evaporation of saturated solutions of freshly recrystallized monomer in acetone or methylbutylketone at 4°C in the dark. The crystals are plate-shaped, with an area of 0.1–1 cm^2, and a thickness of 50–250 μm. They contain a very small amount of polymer chains dispersed in the crystalline monomer matrix, $\sim 10^{-5}$–10^{-4} in weight. Controlled amounts of polymer can be generated by irradiation with low γ-ray doses [4].

3. Experimental results

3.1. Evidence for triplet state formation: TT* photoinduced absorption

A typical PIA spectrum in the near infra-red region at 4 ps after photoexcitation by the pump pulse is shown in Fig. 3. At delay times less than 1 ps, this signal is superimposed on a short-lived broad-band PIA (see inset to Fig. 3). The sharp decrease in the PIA spectrum at 1.33 eV is due to the chirp of the continuum probe pulse; for delay times greater than the pump-probe cross-correlation time the short-lived absorption is featureless throughout the range observed. The dynamics of this short-lived absorption component will be discussed in a subsequent publication in connection with the bleaching of the singlet exciton absorption. For the present work we content ourselves with discussing how we subtract off the short-lived component of the signal to extract the position, width, and magnitude of the TT* absorption. Using a 5th-order polynomial, we fit the raw PIA spectrum (the upper curve of small dots in the inset to Fig. 3) between 1.2 and 1.5 eV, excluding the region between 1.3 and 1.4 eV. This fit is shown in the inset to Fig. 3 as the upper thin solid line and serves as a baseline which is subtracted from the data. The resulting curve is the lower dotted curve in the inset to Fig. 3 and is fitted using a Lorentzian lineshape which is shown as the lower thin solid line. From these fits we extract the magnitude, position and width of the TT* absorption.

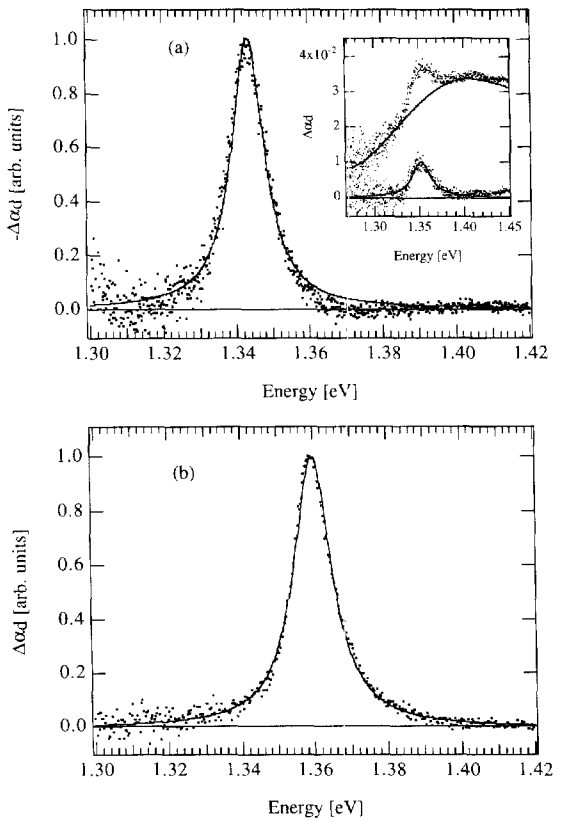

Fig. 3. Panel (a) shows the differential absorption spectrum for PDA-4BCMU 4 ps after photoexcitation by a 150 fs pump pulse. The fit is to a Lorentzian with a fwhm of 12.8 meV, which corresponds to a lifetime of 115 fs for the excited triplet state, assuming homogeneous broadening. The upper dotted curve in the inset is the raw differential absorption signal at a delay time of 100 fs at 1.35 eV and the corresponding solid line is a 5th-order polynomial fit used to estimate the baseline of the broad-band absorption, as described in the text. The lower dotted curve in the inset shows the treated data which result from subtracting the baseline fit from the raw data, and the lower solid curve shows a Lorentzian fit to the treated data. Panel (b) shows the differential absorption spectrum at 4 ps delay time in PDA-3BCMU fit to a Lorentzian with a fwhm of 13.6 meV.

Following excitation in the singlet exciton absorption band, a narrow Lorentzian absorption line is observed in the NIR in 3BCMU and 4BCMU. In 4BCMU at 20 K, the line peaks at 1.345 eV, with a fwhm of 100 cm^{-1} (12.5 meV). The corresponding values for 3BCMU are 1.360 eV and 120 cm^{-1} (13.5 meV) at 20 K, and 1.375 eV and 180 cm^{-1} (22.3 meV) at 77 K. These lines are only slightly broader than the exciton absorption line. The values given above are measured 4 ps after excitation; at earlier times, the absorption line is somewhat broader and slightly blue-shifted. This will be considered further in Section 3.3.

This absorption is likely to be the 0–0 line of an electronic transition, since no other line is found down to 1.20 eV, over a range ≥ 0.15 eV. Vibronic satellites may be present at higher energy, but the quality of the probe continuum becomes increasingly poorer above ~ 1.4 eV, preventing any accurate study.

In all PDAs, including bulk poly-4BCMU [21], a photoinduced absorption is observed around 1.4 eV [15–18]. It has been unambiguously shown to be a

triplet–triplet (TT^*) absorption by studying the effect of microwaves or of a magnetic field, and this absorption has been used in absorption-detected magnetic resonance (ADMR) studies of the PDA triplet state [20]. It therefore seems reasonable to assign the observed induced absorption to the same TT^* transition in the present experiments as well. The absorption will then be used to monitor the triplet population and study its formation and decay.

3.2. Excitation profile of the TT^* absorption

The fluence dependence of the TT^* absorption magnitude was studied at 9 pump wavelengths between the S_1 absorption energy and 2.48 eV. This yields the general trends of triplet generation if not a complete spectrum.

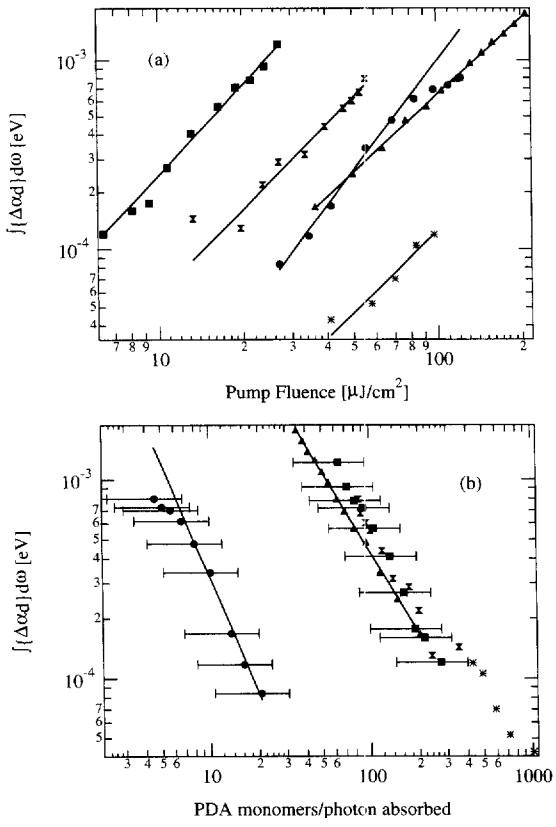

Fig. 4. Panel (a) shows the dependence of the relative oscillator strength (measured as the integral of the differential absorption spectrum) on the pump fluence. The circles correspond to pumping at 1.82 eV, the squares at 2.00 eV, the triangles at 2.09 eV, the hourglasses at 2.14 eV and the stars at 2.42 eV. Panel (b) shows the same data plotted as a function of the number of monomers per photon absorbed. The solid lines in both plots are fits to a power law, with the exponent m given in Fig. 5.

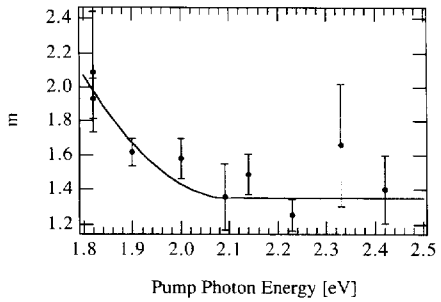

Fig. 5. The dependence of m, which is the exponent obtained from fitting the data in Fig. 4 to a power law in pump intensity (signal I^m), on the pump wavelength, for PDA-4BCMU.

Triplet generation is not a linear function of the pump fluence I (μJ/cm^2 per pulse). I could be varied only over a factor of 5. Over this limited range, the data can be fitted to power laws I^m as shown in Fig. 4. In 4BCMU, $m \approx 2$ at 1.82 eV, the exciton peak, then decreases to values of the order of 1.4 at higher pump photon energies (Fig. 5). Data for 3BCMU also show a general decrease, but with more erratic variations.

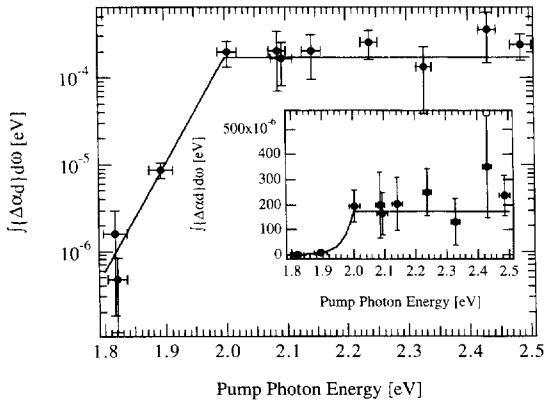

Fig. 6. The relative number of triplets generated at an excitation density of one photon absorbed every 200 monomer units, plotted as a function of pump wavelength for poly-4BCMU. The inset shows the same data plotted on a linear scale. The solid lines are not fits, but only to guide the eye.

Fig. 6 shows the integrated intensity of the induced absorption band 4 ps after the pump pulse, and for the same number of absorbed photons at all wavelengths – fluences such that 1 photon is absorbed for 200 monomer units in the chain – vs. pump photon energy. This gives the variation of triplet generation efficiency vs. pump photon energy. In 4BCMU, the triplet yield increases exponentially by more than two orders of magnitude between S_1 and 2.0 eV, then becomes almost constant up to 2.5 eV, although a slight increase cannot be excluded as shown in the inset of Fig. 6a.

In 3BCMU, the yield at 1.9 eV — the S_1 energy — is also more than one order of magnitude smaller than at higher photon energies.

3.3. Variation of the TT* absorption spectrum during the first few ps

The position and width of the TT* absorption band vary slightly at early times. The transition energy shifts to the red by ~ 5 meV during the first picosecond (Fig. 7a), then becomes almost constant; further redshift up to 50 ps being of the order of 1 meV. Simultaneously, the band significantly narrows from $2\Gamma \approx 20$ meV (fwfm) at $\tau = 0$ to $2\Gamma \approx 12$ meV after 5 ps (Fig. 7b). These changes are very similar for 4BCMU at 20 K and for 3BCMU at 20 and 77 K. The early time variations can be fitted to monoexponentials with time constants of 350 fs and 1.2 ps, respectively. Although there is an overall increase of these shifts with excitation density and pump photon energy, the variations are irregular.

3.4. Triplet decay

The time dependence of the TT* absorption intensity, which is proportional to the triplet exciton population, was measured up to 50 ps by integrating the PIA band at each time delay. The results are shown as open circles in Fig. 8. A triplet lifetime of ~ 50 μs in bulk PDAs has been reported in the literature [16,18,19]. The decay we observe is much more rapid and non-exponential. Since the decay of the triplet population is very fast in our experimental situation, all triplets generated by a pump pulse have decayed well before the arrival of the following pulse.

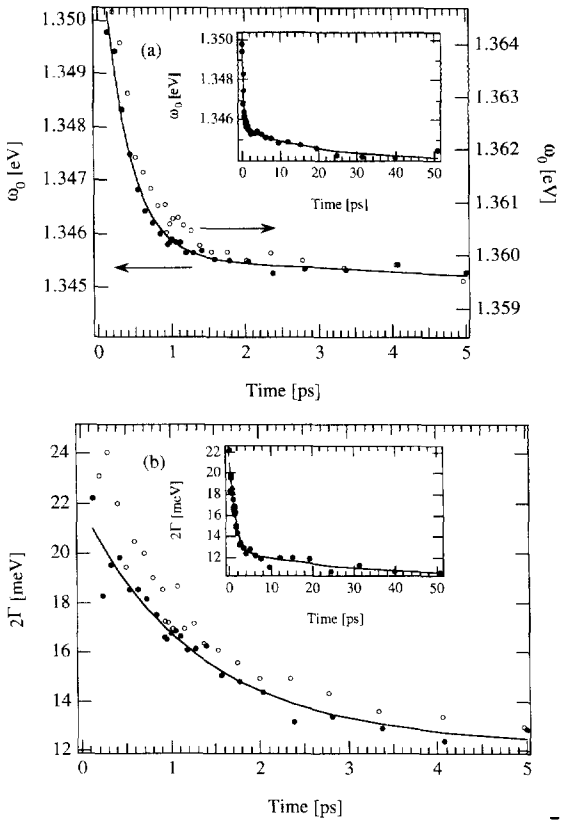

Fig. 7. Panel (a) shows the position of the T–T* absorption as a function of time. The open circles are for PDA-3BCMU (right-hand axis) and the solid circles are for PDA-4BCMU (left-hand axis). The solid lines are double-exponential fits with time constants of 300 ± 50 fs and 20 ± 10 ps. The inset shows the data for PDA-4BCMU to 50 ps delay time. Panel (b) shows the decrease in the linewidth of the T–T* absorption line as a function of time, obtained from fitting the differential absorption spectra to a Lorentzian. The open circles are for PDA-3BCMU, the solid circles for PDA-4BCMU and the solid line is a double-exponential fit to the data for PDA-4BCMU and yields time constants of 1.2 ± 0.2 and 20 ± 10 ps. The inset displays the data for PDA-4BCMU to 50 ps delay time.

As discussed in Section 4.2.2 below, this very fast decay is explained by the fact that in our experiments triplets are created by fission as correlated pairs in a strictly 1-D geometry. A theoretical treatment of this situation, assuming diffusive motion of the triplets and nearest neighbor annihilation, is given in Appendix A. This theory yields satisfactory fits to

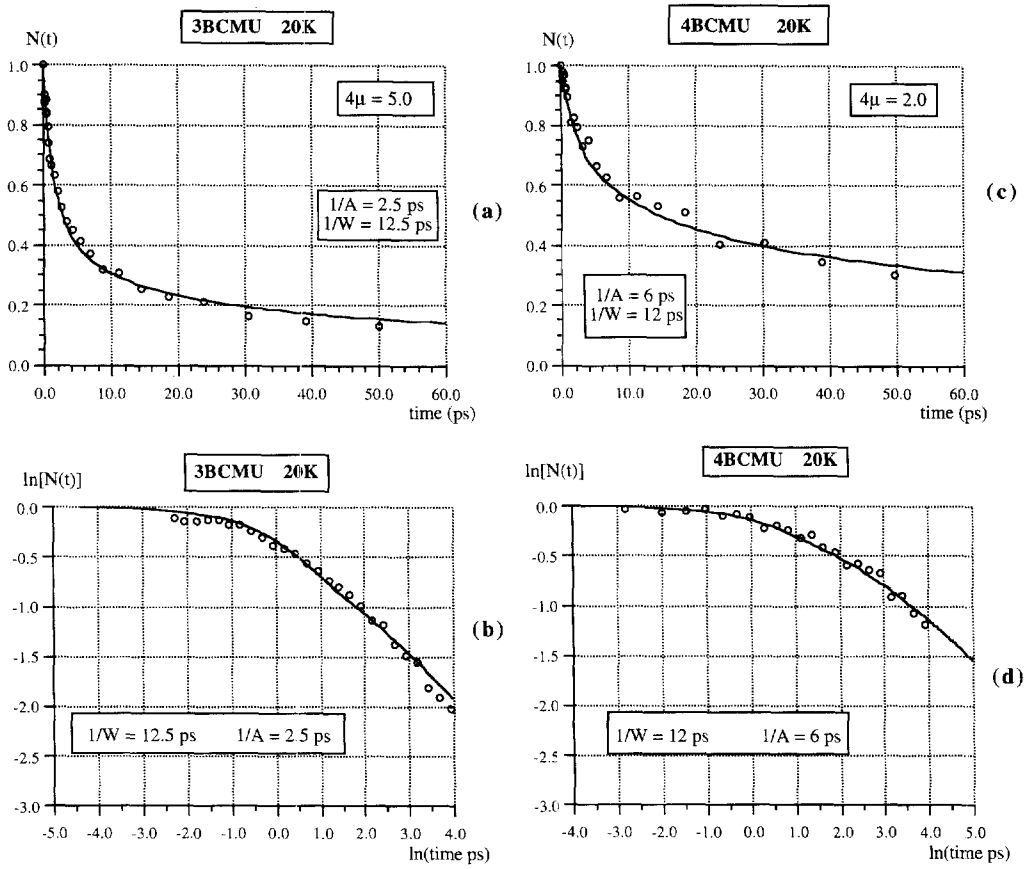

Fig. 8. Experimental time decays of the triplet population and theoretical fits. Open circles are experimental points, normalized to the value at time zero. Solid lines are fits for the indicated values of A and W. Poly-3BCMU at 20 K: (a) linear time scale, (b) logarithmic time scale. Poly-4BCMU at 20 K: (c) linear time scale, (d) logarithmic time scale.

the experimental data as shown in Fig. 8 by the solid lines.

4. Discussion

4.1. Triplet generation

4.1.1. Possible triplet generation processes

Triplet excitons can be generated during the relaxation of a singlet state created by absorption of a pump photon through several processes: intersystem crossing (ISC), which produces a single triplet, or singlet fission, which produces a pair of triplets of total spin zero (Scheme 1).

The probability π_1 of fission from a vibrationally excited singlet exciton S_1^* will vary with pump photon energy, whereas the total probability π_{isc} of intersystem crossing from all excited states will not (the lifetime of S_1^* is too short to allow significant ISC from it).

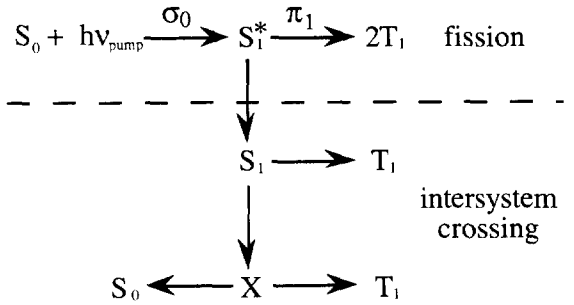

Scheme 1. One-quantum processes for triplet generation from a singlet excited state.

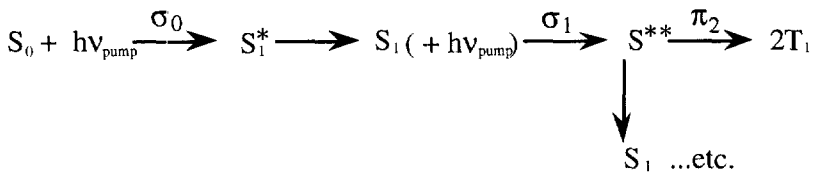

Scheme 2. Triplet generation by photoexcitation of a singlet excited state.

These processes however have different energy requirements. If $E(S)$ is the energy of a singlet state S, the first process requires only that $E(S) > E(T_1)$, which is true for the free singlet exciton S_1 and its vibronic excitations S_1^*, but may also be true of lower lying singlet states X, such as a self-trapped ^1B_u state or an ^1A_g exciton, which may be intermediate states in the singlet exciton energy relaxation scheme. Fission on the other hand requires that $E(S) > 2E(T_1)$. The energy of the exciton state S_1 does not necessarily fulfill this condition, while the higher vibronic excitations S_1^* of the free exciton do. This implies there will be a threshold for fission. In some experiments on PDAs [18,22] this threshold has been found to be above the singlet exciton energy S_1. The intersystem crossing was also found to be very inefficient, probably because ISC is not fast enough to compete with the very rapid non-radiative relaxation of the singlets. ISC rates in the range 10^6 to 10^{10} s^{-1} are found in conjugated molecules [23] and in polymers [24]. It is then generally assumed that in PDAs most triplets are generated by exciton fission.

Both processes shown in Scheme 1 involve one photon only, so the number of generated triplets N_T should be proportional to the pump fluence I. However, what is observed is that N_T is proportional to I^m with $2 > m > 1$. Unfortunately, m is deduced from experiments in which I could be varied over less than one order of magnitude, so the results most probably correspond to the coexistence of a linear and a quadratic process having, in our experimental conditions, comparable yields.

We now consider two possible quadratic processes: the photoexcitation of a singlet excited state by absorption of a pump photon, or the bimolecular interaction of two singlet states. The first one is depicted in Scheme 2.

The different absorptions have different initial states, hence different cross-sections, and in addition these cross-sections will depend on the pump photon energy. Since the pump pulse duration is very short, we shall neglect any triplet generation process by photoexcitation of the states that may be populated by relaxation of the S_1 state.

The second type of quadratic process is the interaction of singlet excitations. Such processes are depicted in Scheme 3.

These processes differ from those shown in Scheme 2 in two respects. First, they depend only on the concentration of excited species, and not on the energy of the pump photons that were used to generate them: the yield should be independent of pump photon energy. Secondly, they may occur during the whole lifetime of the singlet excitations. The states labeled X in Scheme 3, which are produced by relaxation of the S_1 states, have lifetimes in the picosecond range [10,13], so their interaction will

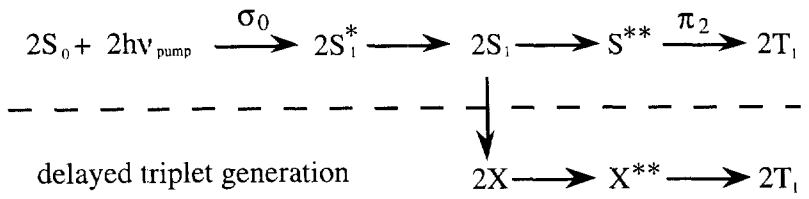

Scheme 3. Triplet generation by interaction of singlet excitations.

lead to 'delayed' generation of triplets, i.e. generation well after the end of the pump pulse.

4.1.2. Evidence for the dominant triplet generation processes: Dependence of the triplet yield on the energy of the initial singlet state.

As already mentioned, the exponent m of the variation of triplet yield with fluence is $m = 2$ at the exciton energy. This demonstrates that neither fission nor intersystem crossing occur at a significant rate at that energy. Therefore, the threshold for fission is above the free exciton energy.

4.1.2.1. One-quantum process. The triplet yield increases rapidly over the first 0.1–0.2 eV above the singlet exciton energy, then stays almost constant — or increases by at most 25% — up to at least 2.5 eV. For 4BCMU, in the energy range between 2 and 2.5 eV, the exponent m of the variation of triplet yield with fluence is ~ 1.5.

A simple calculation shows that if the one- and two-quantum processes have equal yields at a fluence I_0, data recorded for a five-fold fluence variation around I_0 can be fitted with a power law $I^{1.5}$ to better than 10%. Similarly, $I^{1.4}$ corresponds to the one-quantum process yield being 1.5 times that of the two-quantum one, $I^{1.3}$ to a ratio of 2.5, etc.

The results of Fig. 5 therefore indicate that the one-quantum process of exciton fission makes up $\sim 50\%$ of the triplet yield at 2.0 eV. The experimental data do not discriminate between a constant value of $m \approx 1.4$ above 2.1 eV and a slow decrease of m from ~ 1.6 at 1.90 eV to 1.3 at 2.5 eV. As the total fission yield (Fig. 6) increases rapidly up to ~ 2 eV, then very slightly if at all, remaining constant to $\pm 30\%$, the one-quantum fission process yield is almost constant above 2.0 eV, increasing at most by a factor of 2 up to 2.5 eV. We note that a very similar situation was observed in anthracene [25], and over a narrower energy range in tetracene as well [26].

When a high energy exciton state is prepared by photon absorption, fission may occur in parallel with energy relaxation by phonon emission until the residual energy becomes smaller than the fission energy threshold. A possible explanation of the observed behavior is therefore that there is a level near 2 eV with a much higher fission probability than the higher lying ones, and which is an intermediate level in their vibrational relaxation. In such a case, highly lying singlet states would rarely undergo fission before relaxation to the 2 eV state. This increased fission probability may correspond to a state having a larger fission rate, even though that state does not have a particularly long lifetime. One could also consider a state without a particularly large fission rate, but with a much longer lifetime. However, there is no evidence for another electronic state at that energy in our absorption or electroabsorption studies.

4.1.2.2. Two-quantum processes. Two-quantum processes involving bimolecular interaction of excited singlet states involve relaxed excitations, and should not depend on the pump photon energy. Direct generation of singlet excitons by resonance pumping at S_1 should be as efficient as pumping at higher photon energies. The low value of the triplet yield upon pumping at S_1 thus shows that these processes cannot play a significant role in the present experimental conditions. The only two-quantum processes to be taken into account are those involving photoexcitation by the pump pulse of singlet excitons S_1 generated by the same pulse. The short duration of the pump pulse means we need only consider the free excitons and can neglect both the relaxation of S_1 during the pump towards lower lying states, and the photoexcitation of such states There will be no delayed generation of triplets, so the time dependence of the TT^* absorption, which will be analyzed below, will therefore yield the time dependence of the initially created triplet population.

4.1.2.3. The singlet photoexcitation process. In order to demonstrate the plausibility of the singlet photoexcitation process we estimate the yield due to fission of photoexcited singlets S^{**} and compare with an estimate of the yield of vibrationally excited singlets, S_1^*, directly prepared by the pump.

The temporal shape of the pump pulse is given by:

$$\phi(t) = \phi_0 \operatorname{sech}^2(t/\tau) \tag{1}$$

with $\tau \approx 85$ fs. The number of S_1 states (per unit sample surface) present at time t, neglecting their

decay during a time of order τ, and assuming for simplicity an optically thin sample, is given by integrating Eq. (1) as:

$$N_s(t) = \sigma_0 N d \phi_0 \tau [1 + \tanh(t/\tau)], \quad (2)$$

where σ_0 is the cross-section per chain repeat unit for absorption from the ground state, N (cm^{-2}) is the density per unit surface of chain repeat units in the sample, and d is the sample thickness.

During the time interval dt, these singlets absorb $\sigma_1 N_s(t)\phi(t)dt$ photons, where σ_1 is the absorption cross-section for S_1. The total number of such events leading to a photoexcited singlet S^{**} during the entire pump pulse is given by integration over all time to be:

$$\sigma_0 N d \phi_0 \tau \sigma_1 \int \phi(t)[1 + \tanh(t/\tau)]dt. \quad (3)$$

$\int \phi(t)dt = 2\phi_0\tau$, and the integration of the tanh yields zero. If π_2 is the probability that a S^{**} state yields a triplet pair during its relaxation towards S_1, the total number of triplets thus generated during the pump pulse is:

$$4\pi_2(\phi_0\tau)^2 \sigma_0 \sigma_1 N d \quad (4)$$

per unit sample surface.

This is to be compared to the number of triplets directly generated by fission of S_1^* excitons produced by pump photons, which is given as:

$$4\pi_1 \sigma_0 N d \phi_0 \tau. \quad (5)$$

The ratio of Eq. (5) to Eq. (4):

$$\phi_0\tau(\pi_2/\pi_1)\sigma_1 \quad (6)$$

should be of order unity if the yields of the two processes are comparable, so that the exponent of the fluence dependence of the triplet yield is ~ 1.5. π_2/π_1 is certainly larger than one since the energy of the S^{**} states are much higher than that of S_1. A typical value is $\phi_0\tau \approx 3 \times 10^{14}$ photons/cm^2, and σ_1 is given by the photoinduced absorption spectrum. In the present experiments [10], a wide absorption band extends from just above S_1 towards higher energy, and the corresponding cross-section is estimated to be $\sim 10^{-15}$ cm^2. Hence the quantity (6) is indeed of order 1, showing that the two-quantum process depicted in Scheme 2 is indeed comparable in yield to the one-quantum process of Scheme 1.

4.2. The lowest triplet state

4.2.1. Energy of the free triplet exciton

From the variations of the triplet yield with pump wavelength and fluence shown in Figs. 5 and 6, it is possible to obtain information on the energy of the free triplet.

As discussed above in Section 4.1.1, triplets may be generated either by one-quantum processes, linear in pump fluence, or by two-quantum processes, quadratic in fluence. In the present experiments, the dominant linear process is fission of the singlet state S_1^*. This process may only occur from states whose energy is larger than twice the energy of the free triplet state.

Fig. 5 shows that in 4BCMU, the triplet yield is quadratic in fluence upon pumping at the singlet exciton energy 1.82 eV, so no one-quantum process is active at that energy. This gives a lower limit for the free triplet exciton energy $E(T_1)$ which must be larger than half the singlet exciton energy. However, the exponent m of the fluence dependence is already significantly less than 2 at 1.9 eV. This implies that a process linear in fluence, not present at the singlet exciton energy, occurs at 1.9 eV. This cannot be intersystem crossing (ISC), since it would occur at the singlet energy as well. The only possibly important one-photon triplet generation process is fission. The energy threshold for fission is therefore at — or below — 1.9 eV. This gives an upper limit for the free triplet exciton energy at 20 K in poly-4BCMU chains isolated in their monomer crystal matrix, so that:

$0.9\ \text{eV} < E(T_1) \leq 0.95\ \text{eV}$ for poly-4BCMU.

Similarly, it is found that for poly-3BCMU chains at 20 K diluted in their monomer crystal matrix:

$0.95\ \text{eV} < E(T_1) \leq 1.0\ \text{eV}$ for poly-3BCMU.

In both cases, the singlet exciton is less than 0.1 eV below $2E(T_1)$.

We are aware of only one other estimate of the triplet exciton energy in a PDA, in the case of poly-DCH polycrystalline films at room temperature

[18], where $E(T_1) \approx 1.07$ eV. In that PDA, the room temperature singlet exciton energy is 1.90 eV [27], which places the singlet at more than 0.15 eV below $2E(T_1)$.

4.2.2. Triplet transport properties

The photoinduced TT^* absorption decays non-exponentially on a 10 ps time scale (Fig. 8) whereas it is stated in the literature that triplet excitons in PDAs decay exponentially with a lifetime of ~ 50 μs [16,18,19]. For instance, Gass et al. [21] found that the TT^* absorption corresponding to generation of triplets by one-photon near IR absorption in bulk poly-4BCMU crystals does not decay perceptibly on the time scale of 100 ps.

These conflicting observations can be understood if one considers the differences in triplet generation processes and in the dimensionality of the system. In our experiments, triplet excitons are generated by singlet fission, yielding a correlated pair of triplets of total spin zero which is strictly confined on one chain (a 1-D system). In such a situation, non-radiative decay of individual triplets is unimportant compared to repeated triplet–triplet interactions of the correlated triplet pair which lead to a simultaneous decay of both triplets by fusion into a singlet exciton, a process known to have a relatively high efficiency in molecular crystals [28,29].

The experiments reported here were performed at relatively low excitation densities: one absorbed photon per 10^2 to more than 10^3 chain repeat units. Since a poly-4BCMU chain isolated in its monomer matrix contains ~ 5000 units [4], there are less than 50 excitations per chain. Thus, if the fission yield is not more than a few percent, most chains will contain one or zero triplet pairs [30].

We shall assume that triplet motion is diffusive, with a hopping rate W, and that triplet–triplet interaction leading to fusion can take place only between triplets located on the same site, with a rate constant A. At time zero, the two triplets are generated on the same site. Considering the short times involved, spin relaxation effects can be neglected. A similar problem was solved by Torney and McConnell [31] but with different initial conditions: they assumed complete randomness of the initial particle positions.

The analytical solution given in Appendix A may be compared with the observed decay kinetics. The triplet population decay will first display at short times — $t \ll W^{-1}$ — an exponential regime $\exp(-At)$, whereas the long time variation will follow a $t^{-1/2}$ law. This law results from the fact that diffusive motion entails that the distance between two surviving triplets increases as $t^{1/2}$. Since W and A dominate different regions of the decay, both can be determined quite accurately by fitting the data.

Fig. 8a and b shows a typical fit corresponding to poly-3BCMU chains at 20 K. We obtain an excellent agreement over the entire experimental time range using the values $A^{-1} = 2.5$ ps and $W^{-1} = 12.5$ ps.

The high quality of the fit confirms that triplet motion is indeed diffusive. In particular, the $-1/2$ exponent reached at the longer times (≥ 30 ps) can be viewed as the signature of a diffusive process. The dimensionless ratio W/A is obtained with a good accuracy, of the order of a few percent. On the other hand the absolute time scale is given by the initial slope, which is limited by the baseline subtraction procedure (see Fig. 3), so the uncertainty on the absolute values of W and A is larger, of the order of $\pm 20\%$.

Similar fits of decays recorded at 77 K yielded $A^{-1} = 7$ ps and $W^{-1} = 17$ ps. Thus, triplet diffusivity appears to be a slightly decreasing function of temperature. The annihilation rate decreases faster, so the probability of reaction of a triplet pair at contact decreases from ~ 0.7 at 20 K to 0.55 at 77 K.

For poly-4BCMU isolated chains, results were obtained at 20 K only, yielding again very similar values: $A^{-1} = 6$ ps and $W^{-1} = 12$ ps (Fig. 8c and d).

In order to calculate a diffusion coefficient, a hopping distance has to be chosen. The triplet exciton fine structure tensor has been determined in bulk single crystals of a different PDA named pTS [16,19,20]. Its orientation relative to the chain axis direction, and the value of the zero field splittings agree with the triplet being slightly more extended than one chain repeat unit, so we shall assume a hopping distance equal to the length of one repeat unit ~ 5 Å.

A lower limit of the triplet diffusion coefficient $D \approx 10^{-4}$ cm^2 s^{-1} below 80 K is then obtained. To our knowledge, this is the first time that a direct

estimate of an exciton transport coefficient in PDA has been obtained [32].

The analysis also yields a high probability of fusion of two triplets as the ratio $A/(A+2W) \approx 0.7$, which is close to unity. In this limit and in one dimension, the fusion rate constant corresponding to a population of initially spatially uncorrelated triplets would be $\gamma \approx 4\sqrt{(\beta D)}$ cm/s [33], where β is the non-radiative decay rate constant of an isolated triplet. Using the literature value $\beta \approx 2 \times 10^4$ s^{-1} [16,19,20] one gets $\gamma \approx 5$ cm/s.

We are aware of only one work on a PDA in which a triplet fusion rate (actually an upper limit) was estimated [18]. As for all previous experiments on triplets in PDAs, that work used bulk polymer samples; in that case a polycrystalline film. Even though interchain coupling in such samples may be small (and generally is assumed to be so), it is unlikely that it be so small that a triplet exciton will remain confined to the same chain during its entire 50 μs lifetime. In the case of a very anisotropic 3-D motion (quasi-1-D), β should be replaced by the probability of out-of-chain hopping ψ_{out} [33]: $\gamma \approx 4\sqrt{(\psi_{out} D)}$.

Jundt et al. [18] estimated $\gamma \leq 7 \times 10^{-15}$ cm^3 s^{-1}; these units implicitly assume 3-D motion. This is a very small value for 3-D interactions [28,29] implying a very small diffusion coefficient, not compatible with our experimental value of W. However, the two experiments are too different to warrant further discussion of the problem at present.

4.2.3. Occurrence of triplet exciton self-trapping

The above theoretical treatment of the triplet population decay assumes that A and W do not vary in time. This assumption is born out by the fact that the fit is good at all times observed, covering more than two orders of magnitude.

However, small variations of the TT^* PIA spectrum described in Section 3.3 are observed, particularly during the first picosecond. These variations show that there is an evolution of the system on this timescale. The evolution may correspond to at least two types of phenomena: a self-trapping of the triplet, or the gradual relaxation of phonons. Phonons are created during the relaxation of the states prepared by the pump pulse, and their presence on the chain may affect the exciton population.

The small changes observed after 1 ps are very likely due to this phonon relaxation. The situation at earlier times is less clear, and the possibility of triplet self-trapping occurring on the time scale of 300 fs to 1 ps cannot be excluded. It seems however that self-trapping, if present, does not strongly affect the triplet properties. It is possible that the differences in the structure of the free and the self-trapped excitons are not large.

4.3. The excited triplet level T^*

4.3.1. Energy and lifetime of T^*

Upper and lower bounds for the lowest triplet exciton energy were obtained in Section 4.2.1. Adding the TT^* transition energy to these values yields bounds for the position of T^*: for poly-4BCMU isolated chains at 20 K, 2.24 eV $< E(T^*) \leq$ 2.29 eV, and for poly-3BCMU 2.31 eV $< E(T^*) \leq$ 2.36 eV. These values are just below the experimental gap energies, i.e. the valence band-conduction band transition, which are 2.37 eV for poly-4BCMU and 2.48 eV for poly-3BCMU chains [8].

Since the TT^* transition is strongly allowed (see below), T^* must be a ^3A_g state. Hence, our results show the presence of an A_g triplet ~ 0.1 eV below the gap. Such a state is predicted in some theoretical calculations, and an A_g state in that energy range has been found necessary to quantitatively account for the experimental electroabsorption signal corresponding to the gap [34].

The lifetime of the T^* state can be deduced from the experimental width of the Lorentzian TT^* absorption line, assuming that the corresponding time is given by the population decay, which is very rapid. A lifetime ~ 100 fs at 20 K is found. This is a relatively long lifetime for a high lying excited state. Apparently, T^* is only weakly coupled, if at all, with the dense manifold of singlet vibronic states lying in the same energy range.

4.3.2. Strength of the TT^* transition

By comparing the absorbencies in the TT^* absorption band and in the S_1 exciton band, it is possible to obtain some information on the strength of the TT^* transition.

The integrated optical density in the TT^* band is related to the transition oscillator strength or transition moment by:

$$CE(TT^*)^{-1}OD_{max}(TT^*)\Gamma(TT^*) = \sigma_T n_T d, \quad (7)$$

where C is a constant factor depending only on natural constants, E, OD and Γ are the energy, maximum absorption coefficient and fwhm of the TT^* absorption band respectively, σ_T is the corresponding absorption cross-section per triplet state, n_T the volume number density of photogenerated triplets and d the sample thickness.

Similarly for the exciton absorption band:

$$CE(S_0S_1)^{-1}OD_{max}(S_0S_1)\Gamma(S_0S_1) = \sigma_0 Nd, \quad (8)$$

where $\sigma_0 \approx 2 \times 10^{-15}$ cm^2 is the absorption cross-section per chain repeat unit [4], and N the volume number density of such units.

From the pump fluence and the experimental values of $OD_{max}(S_0S_1)$ and d, one can calculate the number n_ϕ of photons absorbed per chain repeat unit. In the present experiments n_ϕ was typically between 10^{-3} and 10^{-1}. The volume density of singlet excitations generated by the pump is then $n_\phi N$ and:

$$n_T = \eta_T n_\phi N, \quad (9)$$

where η_T is the triplet generation yield from such singlets. Finally,

$$\frac{\sigma_T}{\sigma_0}\eta_T n_\phi = \frac{OD_{max}(TT^*)\Gamma(TT^*)E(S_0S_1)}{OD_{max}(S_0S_1)\Gamma(S_0S_1)E(TT^*)}, \quad (10)$$

in which it has been assumed that both transitions have the same, large, Franck–Condon factor. This is likely to be a good approximation, from the available information on the TT^* transition. The corresponding correction should be of order unity.

In a typical experiment on 4BCMU pumped at 2.09 eV, $n_\phi \approx (2 \pm 0.5) \times 10^{-2}$, $OD(TT^*) = 5.6 \times 10^{-2}$, $\Gamma(TT^*) = 10$ meV, $OD(S_0S_1) = 2.6$ and $\Gamma(S_0S_1) = 6.5$ meV, the only significant uncertainty being on n_ϕ. This gives:

$$\frac{\sigma_T}{\sigma_0}\eta_T \approx \frac{50 \times 5.6 \cdot 10^{-2} \times 10 \times 1.35}{2.6 \times 6.5} = 2.2 \pm 0.5. \quad (11)$$

At 2.09 eV, the exponent of the fluence dependence of n_T, $m \approx 1.5$, indicates that fission of one-photon generated singlets S_1^* produces about half the total triplet yield, so $\eta_T \approx 2 \times 2\pi_1$. Then:

$$\sigma_T \approx \frac{\sigma_0}{2\pi_1}. \quad (12)$$

Since triplet generation is certainly not the major singlet relaxation channel, $\pi_1 \ll 1$, so $\sigma_T \gg \sigma_0$.

In their study of poly-4BCMU single crystals, Gass et al. [21] inferred that the TT^* absorption cross-section should be about an order of magnitude higher than the transition from the ground state to the S_1 exciton. The present conclusion is not contradictory with theirs; the ratio might even be larger. If, for instance, $\pi_1 < 10^{-2}$, as in anthracene [25], then σ_T is larger than σ_0 by two orders of magnitude.

Such a large oscillator strength for absorption from excitons is a well-known feature in semiconductors, particularly striking in materials such as CuCl [35–37].

5. Conclusions

The present work has shown that the energy of the lowest triplet state is slightly larger than half the singlet exciton energy.

Triplets are generated by fission from singlet states prepared either by one- or two-quantum processes. The one-quantum process is fission from the state prepared by absorption of one pump photon; it has a threshold near 1.9 eV in 4BCMU and around 2.0 eV in 3BCMU. The two-quantum process is fission of a highly excited singlet state resulting from absorption of one pump photon by a singlet exciton S_1.

Recombination of the triplet pairs thus formed is very fast. The triplet population decay is described in terms of a 1-D diffusive motion of the triplet excitons and annihilation of the correlated triplet pairs.

Theoretical treatment yields a hopping rate of $\sim 10^{11}$ s^{-1} and an annihilation rate of two triplets in contact of a few 10^{11} s^{-1}.

The triplet population was monitored via a strong TT^* absorption line. The final state T^* of this transition is an A_g triplet state which lies less than 0.1 eV below the electron–hole generation gap. This absorption is very strong: we derive a cross-section which is at least one order of magnitude larger than the corresponding quantity for the ground state to singlet exciton absorption.

Acknowledgements

We are very grateful to Dr. J. Berréhar for preparing and characterizing the high quality crystals studied in this work, and to A. Alexandrou, M. Joffre, J.-P. Likforman and G. Rey for their participation in the experiments. We are also very grateful to G. Rey for his participation to setting up the laser source and assistance in the experiments. We gratefully acknowledge the support of a Chateaubriand scholarship for BK.

Appendix A

We sketch here the theoretical framework supporting the statements made in the main text about the dynamics of the triplet population decay. The basic assumptions are that each triplet undergoes diffusive motion individually and that two triplets localized on the same molecule can annihilate to give an excited (singlet) excitation.

The diffusion can be described by a master equation on a 1-D lattice, the sites of which are labeled by the integer n. This master equation provides the dynamical evolution for the probabilities $p_{n,m}(t)$ to find a triplet on site n and another one on site m at time t. Following standard arguments, and considering nearest neighbors hops only, one can write the following:

$$\frac{\mathrm{d}}{\mathrm{d}t}p_{n,m} = -4Wp_{n,m} + W[\,p_{n-1,m} + p_{n+1,m} + p_{n,m-1} + p_{n,m+1}\,] - A\delta_{n,m}p_{n,m}. \quad \text{(A1)}$$

W denotes the hopping probability per unit time (W^{-1} is the diffusion time); if a denotes the lattice spacing, one can define a diffusion constant $D = a^2W$. A is the annihilation rate: this is the probability per unit time that two triplets annihilate when they are in contact ($\delta_{n,m}$ is the Kronecker symbol).

Eq. (A1) can be solved by first introducing the generating function $f(\phi,\psi,t)$ defined as:

$$f(\phi,\psi,t) = \sum_{n,m=-\infty}^{+\infty} \mathrm{e}^{\mathrm{i}n\phi}\mathrm{e}^{\mathrm{i}m\psi}p_{n,m}(t), \quad \text{(A2)}$$

which yields each $p_{n,m}$ by the inverse relation

$$p_{n,m}(t) = \int_0^{2\pi}\frac{\mathrm{d}\phi}{2\pi}\int_0^{2\pi}\frac{\mathrm{d}\psi}{2\pi}\mathrm{e}^{-\mathrm{i}n\phi}\mathrm{e}^{-\mathrm{i}m\psi}f(\phi,\psi,t). \quad \text{(A3)}$$

By subsequently making a Laplace transformation:

$$F(\phi,\psi,z) = \int_0^{+\infty}\mathrm{d}t\,\mathrm{e}^{-zt}f(\phi,\psi,t), \quad \text{(A4)}$$

it is seen that the F function satisfies the following equation:

$$zF(\phi,\psi,z) - f(\phi,\psi,0) = -2W(2-\cos\phi-\cos\psi) - A\int_0^{2\pi}\frac{\mathrm{d}\phi'}{2\pi}F(\phi',\phi+\psi-\phi',z). \quad \text{(A5)}$$

By labeling $n=0$ the site where the pair of triplets is created (at $t=0$), the solution of the preceding equation is:

$$F(\phi,\psi,z) = \frac{G(\phi,\psi,z)}{1 + A\int_0^{2\pi}\frac{\mathrm{d}\phi'}{2\pi}G(\phi',\phi+\psi-\phi',z)} \quad \text{(A6)}$$

with

$$G(\phi,\psi,z) = \frac{1}{z + 2W(2-\cos\phi-\cos\psi)}. \quad \text{(A7)}$$

This being done, it is easy to go back to the physical expectation values. For instance, the total triplet pair population, $N(t)$, is given by:

$$N(t) = \sum_{n,m=-\infty}^{+\infty} p_{n,m}(t) \equiv f(\phi=\psi=0,t) \quad \text{(A8)}$$

which is now known by its Laplace transform $F(\phi = \psi = 0, z)$, Eq. (A6). Explicit Laplace inversion provides the following expression ($\mu = A/4W$):

$$N(t) = \frac{\mu^2 e^{-4(1+\sqrt{\mu^2+1})Wt}}{\mu^2 + 1 + \sqrt{\mu^2+1}} + \frac{2\mu}{\pi}\int_0^{\pi} \frac{\cos^2(x/2)}{\mu^2 + \sin^2 x} e^{-8Wt\sin^2(x/2)} dx .$$

When $A \ll W$, the first term is always negligible and the second one can be approximated in terms of the error function Φ, so that:

$$N(t) \approx [1 - \Phi\sqrt{(2Wt)}\, e^{2Wt} \quad (\mu \ll 1) \qquad (A10)$$

showing that $N(t)$ decays as $t^{-1/2}$ at large times. In contrast, for $A \gg W$, one has approximately:

$$N(t) = \frac{\mu e^{-At}}{\mu + 1} + \frac{2}{\mu}\left[1 + \frac{1}{8W}\frac{d}{dt}\right]\left[e^{-4Wt} I_0(4Wt)\right] \times (\mu \gg 1), \qquad (A11)$$

where I_0 is the ordinary modified Bessel function; this again yields a $t^{-1/2}$ decay at large times, once the transient exponential regime $\sim e^{-At}$ has disappeared.

Indeed, this final power-law behavior eventually occurs for any value of μ, as can be seen by an asymptotic analysis of the full expression (A9), leading to the following asymptotic expansion:

$$N(t) \sim 2\sqrt{\frac{2W}{\pi A^2}}\, t^{-1/2}\left[1 - 2\frac{\sqrt{2\pi W}}{A} t^{-1/2} + \ldots\right] \times (t \gg W/A^2). \qquad (A12)$$

This entails that the pure $t^{-1/2}$ decay at large times is realized for t much larger than W/A^2, all the more since the correction has itself quite a slow decay. At intermediate times, the decay is neither exponential nor governed by a single exponent (see Fig. 9 giving N for $\mu = 0.5$) as a function of the dimensionless variable $T = Wt$.

Note that $dN/dt(t = 0) = A$, as can be seen from the full exact expression (A9) or by coming back to the master Eq. (A1), taking $n = m$ and summing side by side. Thus, the slope at the origin directly gives the annihilation rate A.

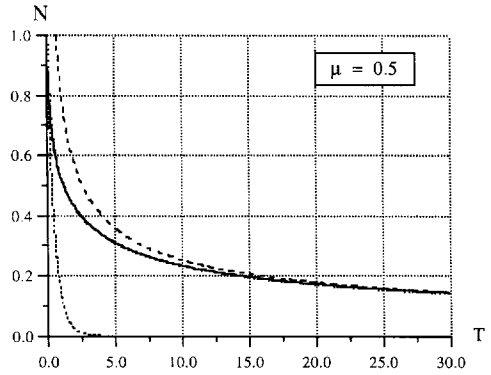

Fig. 9. Theoretical decay of the triplet pair population as a function of $T = Wt$ for $A/4W = 0.5$ (solid line). The dotted line represents the pure exponential decay e^{-At}, whereas the dashed line is the dominant term in Eq. (A12).

Fit with experimental data was achieved as follows: Superposing the experimental and theoretical log–log plots first provides the best value for the dimensionless parameter μ, and also the value of the time scale W^{-1}; this in turn permits the determination of the annihilation rate A. Eventually, self-consistency was checked by comparing the A thus obtained with the initial slope of $N(t)$. As a whole, the accuracy of the absolute values of W and A is probably better than $\pm 20\%$.

References

[1] D. Bloor, R.R. Chance (Eds.), Polydiacetylenes, N. Atlantic Treaty Org., Adv. Stud. Inst. E 102 (Martinus Nijhoff, Dordrecht, 1985).
[2] H.J. Cantow (Ed.) Adv. Polym. Sci. 63 (1984).
[3] M. Schott, G. Wegner, in: D.S. Chemla, J. Zyss (Eds.), Nonlinear Optical Processes of Organic Molecules and Crystals, vol. II, Academic Press, Orlando, FL, 1987, p.1.
[4] S. Spagnoli, J. Berréhar, C. Lapersonne-Meyer, M. Schott, A. Rameau, M. Rawiso, Macromolecules 29 (1996) 5615.
[5] M. Bertault, M. Schott, P. Peretti, P. Ranson, J. Lumin. 33 (1985) 123.
[6] G. Herzberg, Electronic Spectra of Polyatomic Molecules, Van Nostrand, New York, 1966.
[7] S. Spagnoli, J. Berréhar, C. Lapersonne-Meyer, M. Schott, J. Chem. Phys. 100 (1994) 6195.
[8] A. Horvath, G. Weiser, C. Lapersonne-Meyer, M. Schott, S. Spagnoli, Phys. Rev. B 53 (1996) 13507.
[9] C. Lapersonne-Meyer, J. Berréhar, M. Schott, S. Spagnoli, Mol. Cryst. Liq. Cryst. 256 (1994) 423.
[10] B. Kraabel et al., in preparation.
[11] S. Haacke et al., in preparation.

[12] B.I. Greene, J. Orenstein, D.H. Rapkine, S. Schmitt-Rink, M. Thakur, Phys. Rev. Lett. 61 (1988) 325.
[13] T. Kobayashi, Synth. Metals 71 (1995) 1663.
[14] J.Y. Bigot, T.-A. Pham, T. Barisien. Chem. Phys. Lett. 259 (1996) 469.
[15] T. Hattori, W. Hayes, D. Bloor, J. Phys. C 17 (1984) L881.
[16] L. Robins, J. Orenstein, R. Superfine, Phys. Rev. Lett. 56 (1986) 1850.
[17] H. Sixl, W. Rühle, in: J.-L. Brédas, R.R. Chance (Eds.), Conjugated Polymeric Systems, Kluwer, Dordrecht, 1990, p.457.
[18] C. Jundt, G. Klein, J. Le Moigne, Chem. Phys. Lett. 203 (1993) 37.
[19] M. Winter, A. Grupp, M. Mehring, H. Sixl, Chem. Phys. Lett. 133 (1987) 483.
[20] C. Kollmar, W. Rühle, J. Frick, H. Sixl, J.U. von Schütz, J. Chem. Phys. 89 (1988) 55.
[21] P.A. Gass, I. Abram, R. Raj, M. Schott, J. Chem. Phys. 100 (1994) 88.
[22] R.H. Austin, G.L. Baker, S. Etemad. R. Thompson, J. Chem. Phys. 90 (1989) 6642.
[23] N.J. Turro, Modern Molecular Photochemistry, Benjamin, Menlo Park, CA, 1978.
[24] B. Kraabel, D. Moses, A.J. Heeger, J. Chem. Phys. 103 (1995) 5102.
[25] G. Klein, R. Voltz, M. Schott, Chem. Phys. Lett. 16 (1972) 340.
[26] G. Klein, R. Voltz, M. Schott, Chem. Phys. Lett. 19 (1973) 391.
[27] R.J. Hood, H. Müller, C.J. Eckhardt, R.R. Chance, K.C. Yee, Chem. Phys. Lett. 54 (1978) 295.
[28] C.E. Swenberg, N.E. Geacintov, in: J.B. Birks (Ed.), Organic Molecular Photophysics, vol. 1, Wiley, London, 1973, p.489.
[29] M. Pope, C.E. Swenberg, Electronic Processes in Organic Crystals, Oxford University Press, Oxford, 1982.
[30] The chain length of poly-3BCMU chains diluted in their monomer matrix has not been measured yet. However, it is expected that it will be comparable to that of poly-4BCMU, since the respective weight average molecular weights obtained after extensive polymerization are comparable for the two polymers.
[31] D.C. Torney, H.M. McConnell, J. Phys. Chem. 87 (1983) 1941.
[32] An indirect indication of triplet mobility is given by the fact that the calculated hyperfine splitting is larger than the EPR linewidth measured in some cases, indicating the presence of motional narrowing, see Ref. [20].
[33] A. Suna, Phys. Rev. B 1 (1970) 1716.
[34] A. Horvath, Ph.D. Thesis, Philipps-Universität, Marburg, 1996.
[35] E. Hanamura, Solid State. Commun. 12 (1973) 951.
[36] G. Gale, A. Mysyrowicz, Phys. Rev. Lett. 32 (1974) 727.
[37] R.W. Svorec, L.L. Chase, Solid State Commun. 20 (1976) 353.